

Limiting law for ion adsorption in narrow planar pores

D. Bratko*

Department of Chemistry, University of California at Berkeley, Berkeley, California 94720

D. J. Henderson

Utah Supercomputing Institute/IBM Partnership and Department of Chemistry, University of Utah, Salt Lake City, Utah 84112

L. Blum

Department of Physics, University of Puerto Rico, Rio Piedras Campus, San Juan, Puerto Rico 00931

(Received 2 May 1991)

The adsorption of simple electrolytes in narrow planar pores is studied. The validity of the limiting law according to which the density of a classical ionic fluid approaches the fugacity in the pores barely exceeding the diameter of the ions is confirmed using the graphical expansion of the singlet-ion distribution. The same result emerges from the Kirkwood equation for the ion-wall correlation. The analysis is paralleled by the open-ensemble Monte Carlo simulation of the electrolyte in the pore, the periodic boundary conditions being implemented using the two-dimensional Ewald summation. The computations conform with theoretical predictions for extremely narrow slits and provide useful insights into the partitioning of the salt between the slit and the bulk solution at intermediate widths of the pores.

PACS number(s): 68.45.-v, 82.45.+z, 82.70.-y, 82.65.-i

I. INTRODUCTION

While structural studies of electrolyte systems involve inevitable approximations, there are a number of exact criteria that should be met in a satisfactory theoretical framework. Examples are the Stillinger-Lovett moment conditions [1] for interionic distribution in homogeneous solutions, or the contact theorem [2-4] for ion density at rigid interfaces. For neutral surfaces, the latter theorem reduces to a form of the pressure equation regardless of the interparticle pair interaction [4,5]. The present work is concerned with ionic fluids confined by adjacent planar boundaries and with interpenetrating wall-ion distributions. In earlier studies of confined fluids with short-ranged interactions [6-9], an exact limiting law has been derived according to which the number density of the fluid approaches its fugacity at vanishingly small width of the pore. Computer simulations [6-8] and numerical solutions to the anisotropic integral equation approximation conform [10] with this finding. Extensions to ionic systems of the cluster expansion analysis used in the above examples is, however, not straightforward because of the long-ranged nature of the Coulombic interaction. In this study, the expansion of the singlet ion distribution is carried out in terms of the h -bond graphs replacing the f -bond graphs of the former work [6-8] since the screening effects [11] are easier to handle in this representation. The analysis is paralleled by the open-ensemble computer simulation carried out on the restricted-primitive-model (RPM) electrolyte [12] in a slit maintaining equilibrium with homogeneous solution. The distribution of the salt between the bulk phase and the pore is studied. In wide pores, virtually independent adsorption layers are formed at each boundary, the density at the surfaces being determined by the contact theorem [2-4] and therefore by the

osmotic pressure of the solution [4,5,13]. In very narrow pores, barely exceeding the size of the ions, the electrolyte density is found to follow the above limiting law and thus to approach the ionic fugacity of the solution. In either of the two extremes, namely the very wide or very narrow slits, the interfacial density of the salt is determined by thermodynamic coefficients of the bulk solution: the osmotic coefficient in the case of wide pores and the activity coefficient in very narrow pores. The two coefficients can differ significantly from each other and may even deviate from unity in the opposite directions. An interesting dependence of the electrolyte density on the width of the pore is observed in the intermediate width regime for which only approximate theories are available [14,15].

The cluster expansion analysis for the distribution of a classical ionic fluid in a thin layer, virtually squeezed to a two-dimensional region, is outlined in Sec. II. In Sec. III, the grand canonical ensemble Monte Carlo simulation (GCEMC) is described, particular attention being paid to the periodic boundary conditions in this semi-infinite system. Section IV contains simulation results for electrolyte partition between the pore and the bulk solution. A comparison with the prediction of the squeeze limit theorem is made and the dependence of the mean density on the width of the slit is discussed. The mean potential energy of the ions in narrow slits is also considered.

II. GRAPHICAL EXPANSION OF IONIC DENSITY IN A NARROW SLIT

Consider an equilibrium between the solution of a symmetrical salt with bulk ionic number densities $n_+ = n_- = n_b$, and ionic fugacities $\xi_+ = \xi_-$, and a layer of the fluid confined by adjacent hard walls, parallel to

the plane x - y and located at $z = \pm L/2$. Here, the walls are defined as the planes bounding the region accessible to the centers of the ions. The walls are not charged and the permittivity is ϵ uniformly for the entire system. We study the RPM for which the ions are of equal diameter σ . The ion-ion pair potential consists of the hard-core repulsion and the Coulomb interaction

$$u_{ij}(r_{ij}) = \begin{cases} \infty & \text{if } r_{ij} < \sigma \\ Z_i Z_j e_0^2 / 4\pi\epsilon r_{ij} & \text{if } r_{ij} \geq \sigma, \end{cases} \quad (1)$$

where e_0 is the elementary charge, $Z_+ = -Z_-$ the valence of the ions, and r_{ij} the radial distance. Neglecting the quantum effects (that should be present for finite mass particles in very narrow slits [16]), we write for the singlet density of ionic species i , $n_i(1)$ [17]:

$$\ln[n_i(1)/\tilde{n}_i(1)] = C_i(1), \quad (2)$$

where

$$\tilde{n}_i(1) = \tilde{n}_i \exp[-\beta u_i(1)], \quad (3)$$

where $\beta = 1/kT$, k is Boltzmann's constant, T is the temperature, and $u_i(1) = u_i(\mathbf{r}_1)$ is the external potential. Since, for the time being, we will study neutral walls, we take

$$u_i(1) = \begin{cases} 0 & \text{if } |z_1| \leq L/2 \\ \infty & \text{otherwise.} \end{cases} \quad (4)$$

We aim to show that, in the squeeze limit $L \rightarrow 0$, the

function $C_i(1)$ is zero. As was shown in our previous works [6,7], it can be expressed as a series in the fugacity with graphs with f bonds defined by

$$f_{ij}(r_{ij}) = \exp[-\beta u_{ij}(r_{ij})] - 1. \quad (5)$$

However, the Coulomb potential, Eq. (1), yields divergent integrals and the theorem cannot be proven this way. There is an alternate expansion for $C_i(1)$

$$C_i(1) = \textcircled{1} + \textcircled{1} \textcircled{1} + \dots, \quad (6)$$

where the black circles represent density factors $n_j(\mathbf{r}_j)$ and integrals over \mathbf{r}_j , with summation over j . The white and black circles are linked by $h^{(n)}$ bonds where $h^{(n)}$ is the n -particle correlation function. We consider the lowest-order term with the $h^{(2)}$ bond, the pair correlation function $h_{ij} = g_{ij} - 1$. In the case of an ionic fluid confined by planar boundaries [18,19], Jancovici has shown that the pair correlation function has a long-range tail of the form

$$\lim_{r_{12} \rightarrow \infty} h_{ij}(r_{12}; z_1, z_2) = A_{ij} r_{12}^{-3}; \quad z_1, z_2 \rightarrow 0. \quad (7)$$

This rule should be true for a slit containing a neutral mixture of equal size ions. Intuitively, one should think of this mixture in the squeeze limit as a mixture of random dipoles. We now compute the leading graph of Eq. (6), $J_i(1)$, in the limit of a narrow slit $L \rightarrow 0$,

$$\begin{aligned} J_i(1) = \textcircled{1} &= \int d\mathbf{r}_2 \sum_j n_j(\mathbf{r}_2) h_{ij}(r_{12}) \exp[-\beta u_j(z_2)] \\ &= 2\pi \int_{-L/2}^{L/2} dz_2 \sum_j n_j(z_2) \int_{|z_{12}|}^{\infty} dr_{12} r_{12} h_{ij}(r_{12}; z_1, z_2). \end{aligned} \quad (8)$$

From the asymptotic behavior we know that

$$h_{ij}(r_{12}; z_1, z_2) = -\Theta(-r_{12} + \sigma) + \Theta(\sigma - r_{12}) [f_{ij}(r_{12}; z_1, z_2) + A_{ij} r_{12}^{-3}]. \quad (9)$$

Here, (1) denotes $\mathbf{r}_1, \mathbf{r}_{12} = \mathbf{r}_2 - \mathbf{r}_1$, $r_{12} = |\mathbf{r}_{12}|$, and $h_{ij}(r_{ij}; z_i, z_j) = g_{ij}(r_{ij}; z_i, z_j) - 1$ is the total correlation function for the species i and j at the distance r_{ij} , when a particle i is located at the distance z_i and the particle j at the distance z_j relative to the walls. $\Theta(x)$ is the Heaviside step function and $f_{ij}(r_{12}; z_1, z_2)$ is the short-ranged part of $h_{ij}(r_{12}; z_1, z_2)$. The integral $J_i(1) = J_i(z_1)$ of Eq. (8) can now be split to three separate contributions

$$\begin{aligned} J_i(z_1) &= -2\pi \int_{[-L/2, z_1 - \sigma]}^{[L/2, z_1 + \sigma]} dz_2 \sum_j n_j(z_2) \int_{|z_{12}|}^{\sigma} dr_{12} r_{12} \\ &\quad + 2\pi \int_{-L/2}^{L/2} dz_2 \sum_j n_j(z_2) \int_{[z_{12}, \sigma]}^{\infty} dr_{12} r_{12} f_{ij}(r_{12}; z_1, z_2) + 2\pi \int_{-L/2}^{L/2} dz_2 \sum_j n_j(z_2) A_{ij} \int_{[z_{12}, \sigma]}^{\infty} dr_{12} r_{12}^{-2} \end{aligned} \quad (10)$$

or

$$J_i(z_1) = J_i^{(1)}(z_1) + J_i^{(2)}(z_1) + J_i^{(3)}(z_1). \quad (11)$$

Integrating over r_{12} we obtain

$$J_i^{(1)}(z_1) = -\pi \int_{[-L/2, z_1 - \sigma]}^{[L/2, z_1 + \sigma]} dz_2 \sum_j n_j(z_2) (\sigma^2 - z_2^2) \quad (12)$$

and

$$\begin{aligned} J_i^{(3)}(z_1) &= -2\pi \int_{-L/2}^{L/2} dz_2 \sum_j n_j(z_2) A_{ij} \\ &\quad \times [|z_{12}|^{-1} \Theta(z_{12} - \sigma) + \sigma^{-1} \Theta(\sigma - z_{12})] \\ &\rightarrow -2\pi L \sigma^{-1} \sum_j A_{ij} n_j^{(0)}, \end{aligned} \quad (13)$$

and we know that the integral $J_i^{(2)}(z_1)$ is convergent since $f_{ij}(r_{ij}; z_i, z_j)$ is short ranged. When the integration interval $-L/2 \leq z_2 \leq L/2$ becomes sufficiently narrow, all the contributions to $J_i(z_1)$ vanish. We assume that the same will happen to all remaining graphs. Then, in the limit $L \rightarrow 0$,

$$\lim_{L \rightarrow 0} C_i(1) = 0 \quad (14)$$

and

$$\begin{aligned} u_i(z_1) &= 2\pi \int_{-L/2}^{L/2} dz_2 \sum_j n_j(z_2) \int_{[\sigma, z_{12}]}^{\infty} dr_{12} r_{12} h_{ij}(r_{12}; z_1, z_2) u_{ij}(r_{12}) \\ &= (Z_i e_0^2 / 2\epsilon) \int_{-L/2}^{L/2} dz_2 \sum_j n_j(z_2) Z_j \int_{[\sigma, z_{12}]}^{\infty} dr_{12} [f_{ij}(r_{12}; z_1, z_2) + A_{ij} r_{ij}^{-3}]. \end{aligned} \quad (16)$$

The range of the integrand in Eq. (16) is even shorter than in the case of $J_i(z_2)$ in Eq. (10). The mean potential energy of a confined ion tends to zero when the pore width approaches the size of the ions, i.e., when $L \rightarrow 0$. In view of this observation, the Kirkwood integral equation [20] for wall-ion distribution, expressed in terms of the ionic potential energy in the imaginary charging process, represents another route to the limiting law discussed in this section.

III. GRAND CANONICAL ENSEMBLE SIMULATION

The distribution of the RPM salt between the slit and the bulk solution at fixed chemical potential was studied by using the GCEMC procedure that was essentially equal to the method of Valleau and Cohen [21], here adapted to inhomogeneous systems. A detailed description of the method is given in the original work [21] and applications to confined systems have been discussed recently [22,23]. The main difference between the simulation technique of these works [21–23] and our study stems from the particular geometry considered in the present treatment. The planar slit of infinite width in the directions x and y , confined by planar walls at $z = \pm L/2$, is represented by a two-dimensional array of equal,

$$n_i(0) = g_i(0), \quad (15)$$

the number density of the ions approaches their fugacity in vanishingly narrow slits.

Analogous considerations lead to an estimate of the mean potential energy of an ion i due to the interactions with the ionic lamina in the slit. Assuming the electroneutrality of the system, $\sum_i n_i Z_i = 0$, the mean energy of an ion i located at z_1 may be expressed as

periodically repeating cells, each containing the same configuration of the ions [24–26]. In the simulation, only the central cell of volume $V = L_{xy}^2 L$ is considered in an explicit manner while all the replicas are taken into account in energy calculation. The configurational energy U_N of a cell with N ions is given by

$$U_N = \frac{1}{2} \sum_{i=1}^N \sum_{j=1}^N \sum_{\mathbf{P}}' \frac{Z_i Z_j e_0^2}{4\pi\epsilon |\mathbf{r}_{ij} + \mathbf{P}|}. \quad (17)$$

The sum over \mathbf{P} includes all lattice points with the coordinates $\mathbf{P} = (lL_{xy}, mL_{xy}, 0)$ where l and m are integers and the prime denotes the omission of the self-term ($i = j$) in the basic cell with $\mathbf{P} = (0, 0, 0)$ [27]. The infinite summation over \mathbf{P} is carried out using the method of Ewald, adapted to two-dimensional periodic conditions [24,25]. The energy U_N is calculated according to the equations

$$\begin{aligned} U_N = \frac{1}{2} \sum_{i=1}^N \left[\sum_{j=1}^N [u_{ij}^{(1)}(\mathbf{R}_{ij}) + u_{ij}^{(2)}(\mathbf{R}_{ij}) \right. \\ \left. + u_{ij}^{(3)}(\mathbf{R}_{ij})] + u_i^{(4)} \right] \end{aligned} \quad (18)$$

with

$$u_{ij}^{(1)}(\mathbf{R}_{ij}) = (Z_i Z_j e_0^2 / 4\pi\epsilon) \sum_{\mathbf{P}}' \operatorname{erfc}(-\kappa R_{ij}) / R_{ij}, \quad (19)$$

$$\begin{aligned} u_{ij}^{(2)}(\mathbf{R}_{ij}) = (Z_i Z_j e_0^2 / 4\pi\epsilon L_{xy}^2) \sum_{\mathbf{k} \neq 0} \exp(i\mathbf{k} \cdot \mathbf{r}_{ij}) / k [\exp(k|z_{ij}|) \operatorname{erfc}(k/2\kappa + \kappa|z_{ij}|) \\ + \exp(-k|z_{ij}|) \operatorname{erfc}(k/2\kappa - \kappa|z_{ij}|)], \end{aligned} \quad (20)$$

$$u_{ij}^{(3)}(\mathbf{R}_{ij}) = -(Z_i Z_j e_0^2 / 2\pi\epsilon L_{xy}^2) [z_{ij} \operatorname{erf}(\kappa z_{ij}) + \exp(-\kappa^2 z_{ij}^2) / (\sqrt{\pi\epsilon})], \quad (21)$$

$$u_i^{(4)} = -Z_i^2 e_0^2 \kappa / 2\sqrt{\pi}, \quad (22)$$

where $\mathbf{R}_{ij} = \mathbf{r}_i - \mathbf{r}_j$, $R_{ij} = |\mathbf{R}_{ij}|$, \mathbf{k}_{ij} is the two-dimensional reciprocal lattice vector, $k_{ij} = |\mathbf{k}_{ij}|$, $\mathbf{r}_{ij} = (x_{ij}, x_{ij})$, $z_{ij} = z_i - z_j$, and κ is the screening parameter of the Gaussian distributions introduced in Ewald method [29]. The simulation parameters were adjusted to ascertain the average number of 50–100 ions per cell. The moves of randomly chosen ions were attempted with the probability $P=0.5$ and the additions or deletions with the probabilities $(1-P)/2=0.25$. Depending on the concentration, the ion charge, the width L , and other conditions, the maximum displacement was adjusted to keep the mean acceptance of the moves within 40–60%. As usually, the screening parameter κ and the number of the reciprocal \mathbf{k} vectors were chosen in such a way that only the direct interactions of ion i with ion j or with its nearest image, whichever closer, had to be considered in $u_{ij}^{(1)}$. The number of the two-dimensional reciprocal vectors \mathbf{k} was usually 56, this corresponding to about 3×10^2 \mathbf{k} vectors in the three-dimensional Ewald summation. The screening parameter κ was chosen with regard to the cell size L_{xy} according to the relation $\kappa = 4/L_{xy}$ in most of the simulations. A few runs, however, have been made with different values of the above parameters to verify that the result was sufficiently independent of the particular choice within a broader range considered.

IV. RESULTS AND DISCUSSION

The dependence on the pore width of the electrolyte distribution between the bulk phase and the slit was examined to test the prediction of the limiting law of Sec. II and to monitor the intermediate situations with the slit width of up to 4–6 ionic diameters. The RPM parameters were taken from previous studies of bulk solutions. Mono- and divalent RPM electrolytes with ion size $\sigma = 0.425$ or 0.42 nm were considered at the temperature $T = 298$ K and the permittivity $\epsilon = 78.5$ [21,28]. The properties of the solution including some of the known thermodynamic coefficients [20,21,28] are listed in Table I. The width of the pores varied from 5×10^{-4} to about 2–2.5 nm. This was not quite enough for the average properties of the confined solution to become equal to the bulk ones, but the two-dimensional Ewald summation has turned out to be too time consuming to allow the treatment of essentially larger samples. The bulk conditions were, however, correctly recovered when the three-dimensional periodic conditions were imposed and the corresponding Ewald algorithm [29] applied to test the GCCEM procedure against the known results from the literature [21,30].

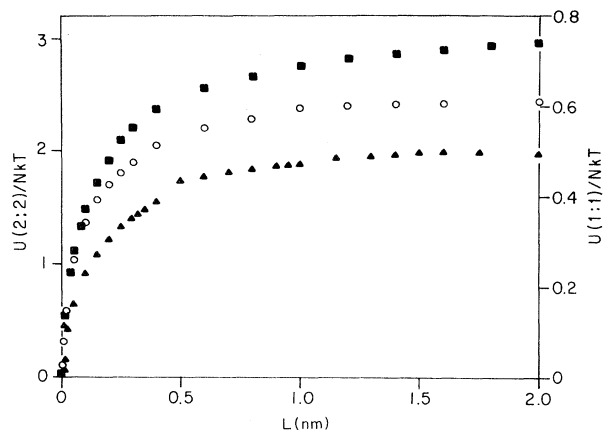


FIG. 1. The mean potential energy of an ion confined in a slit of width L in equilibrium with the bulk monovalent salt solution of concentration $c = 1.0001 \text{ mol dm}^{-3}$ (\circ), $c = 1.9676 \text{ mol dm}^{-3}$ (\triangle), and divalent salt solution at concentration $c = 0.971 \text{ mol dm}^{-3}$ (\blacksquare).

Before turning attention to the pore-solution partition of the salt, we first consider the dependence of the interionic configurational energy on the distance between the walls. In Fig. 1, the decrease in the reduced mean energy of an ion $\langle U_N / NkT \rangle$ accompanying the narrowing of the gap is given for three situations in which the bulk solution contained the 1:1 electrolyte at the concentration 1 or 2 mol dm^{-3} , and the 2:2 electrolyte at the concentration 0.971 mol dm^{-3} . In all the three examples, the reduced energy decreases in a similar manner. It vanishes in extremely narrow pores. The decay is somewhat slower than might have been expected from simply discounting the volume unavailable for the formation of a spherical ionic atmosphere due to the presence of the walls. In vanishingly narrow gaps, the overall mean interaction among the ions becomes insignificant and the confined solution approaches the ideal behavior suggested by Eqs. (15) and (16). The dependence of U_N / NkT on L is rather smooth, although some layering of the ions against the walls could be expected. It should be noted that the mean ionic energy was approximated by the ratio of separate averages $\langle U_N \rangle$ and $\langle N \rangle$ instead of obtaining the mean value $\langle U_N / N \rangle$ in an independent averaging procedure. In view of the fluctuations in U_N and N , the uncertainty in estimated $\langle U_N / N \rangle$ possibly exceeds the errors in the average energy and the number of the ions.

In Figs. 2–6, the mean density of the ions in the pore

TABLE I. The bulk properties of the RPM electrolytes considered in the GCCEM simulations of confined solutions.

System	Valency	σ (nm)	c (mol dm^{-3})	$\ln \gamma_{\pm}$	φ	$-U_b / NkT$
1	1:1	0.425	0.103 76	-0.2311	0.9451	0.274
2	1:1	0.425	1.000 1	-0.1265	1.094	0.552
3	1:1	0.425	1.967 6	0.2545	1.346	0.651
4	2:2	0.420	0.045 6	-1.437	0.64	1.774
5	2:2	0.420	0.971	-2.635	0.605	3.102

$\langle n \rangle$ is shown as a function of the width L at various concentrations of the bulk solution. In wide pores, the mean densities slowly approach the bulk values with increasing L . Considering the thickness of the adsorption layer of the electrolyte at a neutral interface [13,27,31], wider gaps than those studied here would be needed for the surface effects to become insignificant in the solutions with the osmotic coefficient φ considerably differing from the ideal value. In the opposite extreme, with the pore width barely exceeding the size of the ions, the ion density in the slit attains the value close to the fugacity of the ions $\bar{n}_{\pm} = n_b y_{\pm}$. The fugacities are marked by the arrows on the ordinate. With the monovalent salt, Figs. 2–5, the limiting law of Eq. (15) is satisfied within $0\text{--}\pm 2\%$ of the final density. With divalent ions, the absolute agreement is about as good as in the monovalent cases, but the relative deviations are somewhat larger because the limiting densities are so low in these cases. The errors of the GCEMC procedure such as is used in our work are usually around a few percents and our subaverage estimate [32] indicates a possible inaccuracy of up to $\pm 2\%$ of the mean density in the pore. The uncertainty in the activity coefficient y_{\pm} from the literature may be of similar magnitude [21,30], but does not contribute to the deviation from the prediction of the limiting law, Eq. (15), since the fugacity is used as an input for the simulation. On the whole, the GCEMC results confirm the predictions of Sec. II and Eq. (15). In all the cases considered, the limiting density of the ions in the pore lies close to the ionic fugacity, eventual fluctuations around it being of the magnitude expected with the method applied. A computational verification of the narrow pore limiting law for fluids with long-ranged Coulombic interaction is therefore provided.

The dependence of the mean ionic density in the pore on the separation between the walls L is also of interest. As mentioned earlier, the density of the ions next to the walls depends on various factors. With the walls far

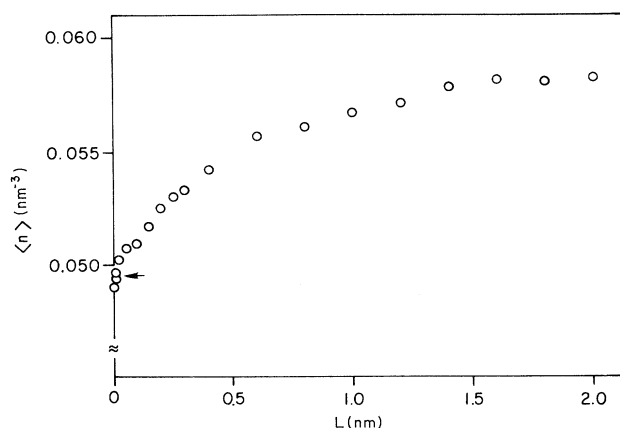


FIG. 2. The mean number density of the ions in a slit of width L in equilibrium with the monovalent salt solution of concentration $c=0.10376 \text{ mol dm}^{-3}$. The arrow denotes the fugacity of the ions.

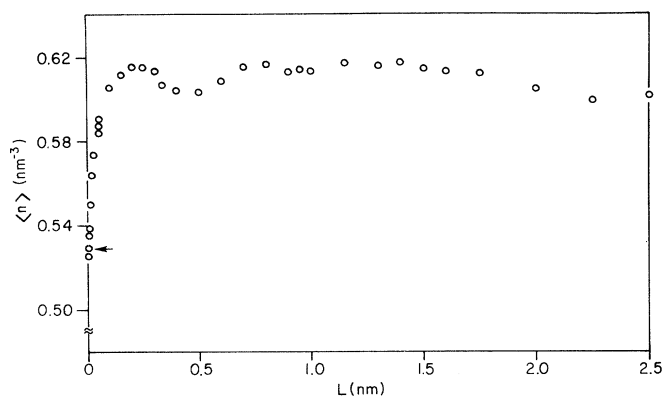


FIG. 3. The mean number density of the ions in a slit of width L in equilibrium with the monovalent salt solution of concentration $c=1.0001 \text{ mol dm}^{-3}$. The arrow denotes the fugacity of the ions.

apart, the contact density is related to the bulk value by the osmotic coefficient of the solution. When bringing the walls closer to each other, a partial superposition of the two wall-ion profiles is possible. In very narrow pores, however, the mean density begins to approach the fugacity, determined by the mean activity coefficient of the ions. When the two coefficients φ and y_{\pm} are of a similar value, a monotonous transition between different regimes is observed. The same holds true if the deviation of y_{\pm} from unity is larger, but of the same sign as with the osmotic coefficient. Both divalent salt examples, systems 4 and 5, belonging to this class, display a monotonous increase in the mean density with widening the gap. A more interesting behavior is observed in concentrated monovalent salt solutions, systems 2 and 3. In the 1-mol dm^{-3} solution, the mean activity coefficient y_{\pm} is lower and the osmotic coefficient φ higher than unity.

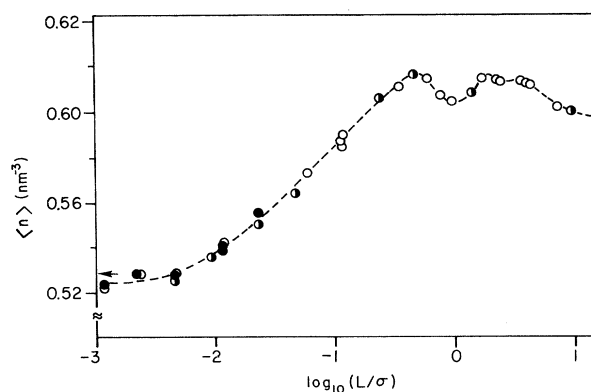


FIG. 4. Same as Fig. 3 but with logarithmic scale for L . The black circles correspond to the simulations with increased number of reciprocal vectors in Ewald summation. The half-solid circles denote the results obtained with a 4–5 times bigger number of ions than in typical runs.

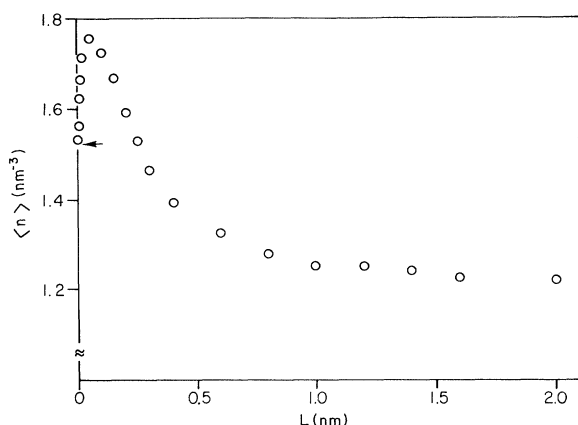


FIG. 5. The mean number density of monovalent ions in a slit of width L in equilibrium with $1.9676 \text{ mol dm}^{-3}$ bulk solution. The arrow denotes the fugacity of the ions.

With the walls sufficiently apart, the mean density in the pore exceeds the bulk value. In analogy with simple liquids [6–10], weak oscillations in the mean density are found when varying the width of the gap, the period being close to the thickness of an ionic monolayer in the pore. In addition to the fact that the mean density exceeds the bulk value, this is another indication of an important role of the hard-core packing effects on the structure of the system. After the distinct maximum observed at the width $L \sim \sigma/2$, the mean density monotonically decays upon narrowing the gap. The rapid drop of the density over a relatively narrow range of L is easier to visualize using the logarithmic scale used in Fig. 4. The narrow gap limit appears to be attained at the smallest values of L , no further decrease being expected with even narrower slits. A check of the applied boundary condi-

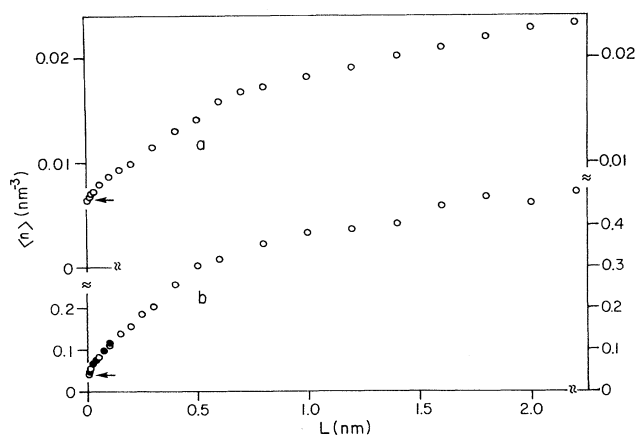


FIG. 6. The mean number density of divalent ions in the gap of width L in equilibrium with the bulk solution of concentration (a) $c = 0.0456 \text{ mol dm}^{-3}$ and (b) $c = 0.971 \text{ mol dm}^{-3}$. Solid symbols correspond to the 4–5 times bigger samples. The arrows denote the fugacities of the ions.

tions is also illustrated. The black circles corresponding to 212 \mathbf{k} vectors in the sums of Eq. (20) agree well with the results obtained by using the lower number of 56 reciprocal vectors \mathbf{k} . Note that these values correspond to essentially higher numbers of \mathbf{k} vectors encountered in an equivalent three-dimensional Ewald summation. Another test was made to examine eventual effect of the size of the system. The half-solid circles denote the results obtained using about 4–5 times larger Monte Carlo cells and numbers of ions. The good agreement with the results obtained with usual samples seems reassuring in this respect.

Figure 5 illustrates the dependence on L of the mean ionic density in the pore in equilibrium with the $1.976 \text{ mol dm}^{-3}$ monovalent salt solution. The high value of the osmotic coefficient $\varphi = 1.346$ of this system reflects notable hard-core exclusion effects present in concentrated solutions. Like in noncharged inhomogeneous fluids, the short-ranged repulsion among the particles leads to the accumulation of the ions at the interface. In analogy with hard-sphere systems [6,10,33], this increase becomes even more pronounced in systems with overlapping adsorption layers. The maximum value of the mean density between adjacent walls is considerably higher than the contact density found at an isolated interface. An opposite effect of weakening the electrostatic interaction between the ion and its truncated ionic atmosphere also exists. According to Fig. 1, the mean potential energy of confined ions rapidly decreases upon reducing L below $\sim \sigma/2$. At sufficiently small distance, this effect takes over and the density is found to pass through a maximum and to decrease upon further narrowing of the pore. In the limit $L \rightarrow 0$, the density attains the value of the ionic fugacity, which in this case exceeds the density of the bulk solution. A rather monotonic decay of $\langle n \rangle$ with L is observed at the separations L beyond the position of the maximum, although some packing effects analogous to those of system 2 would be expected. There may, of course, exist an indistinct oscillating contribution that would be more visible in the absence of the rapid overall decay of $\langle n \rangle$ with increasing L . A similar reasoning applies to the concentrated 2:2 salt solution, Fig. 6, where the rapid growth of $\langle n \rangle$ from $n_b y_{\pm}$ to n_b may hide eventual layering effects. In any case, the latter are less pronounced in the divalent salt solutions in which the electrostatic interactions dictate a considerable reduction in the interfacial density of the ions. The development of an exact analytic theory for ion distribution between adjacent walls at finite separations is not expected in the near future. Quite accurate numerical schemes, however, have become available in recent years [14,34]. It would undoubtedly be of interest to apply these methods to the systems considered in the present study. Extensions of both the theoretical considerations of Sec. II and simulations or inhomogeneous integral equations to systems with polarizable or electrified interfaces are also inviting.

ACKNOWLEDGMENTS

D.B. acknowledges the hospitality of the Utah Supercomputing Institute (USI)/IBM Partnership and the

Department of Chemistry, University of Utah, and the Department of Physics, University of Puerto Rico, where parts of this work were carried out. Financial support from IBM Salt Lake City, Utah, and the National Science Foundation, provided under Grant No. CHE-89-01597 and through the international grant No. INT-

8711845 is acknowledged. Grant No. INT-8711845 is acknowledged. Most of the computations were performed on the IBM 3090/600/6V computer at USI, which is funded by the State of Utah and the IBM Corporation. D.B. and D.H. are grateful to USI for the generous allocation of computer time.

*On leave from University of Ljubljana, Ljubljana, Slovenia.

- [1] F. H. Stillinger and R. Lovett, *J. Chem. Phys.* **49**, 1991 (1968).
- [2] D. Henderson and L. Blum, *J. Chem. Phys.* **69**, 5441 (1978); **75**, 2055 (1981).
- [3] D. Henderson, L. Blum, and J. L. Lebowitz, *J. Electroanal. Chem.* **102**, 315 (1979); D. A. McQuarrie, W. Olivares, D. Henderson, and L. Blum, *J. Colloid Interface Sci.* **77**, 272 (1980).
- [4] H. Wennerström, B. Jönsson, and P. Linse, *J. Chem. Phys.* **76**, 4665 (1982).
- [5] D. Bratko, *Chem. Phys. Lett.* **96**, 263 (1983).
- [6] M. S. Wertheim, L. Blum, and D. Bratko, in *Proceedings of the Symposium on Chemical Physics of Colloidal Phenomena, 189th ACS Meeting, Miami, 1985: Micelles and Microemulsions. Structure, Dynamics and Statistical Thermodynamics*, edited by S. H. Chen and R. Rajagopalan (Springer, New York, 1990), p. 99.
- [7] A. Luzar, D. Bratko, and L. Blum, *J. Chem. Phys.* **86**, 2955 (1987).
- [8] D. Bratko, L. Blum, and M. S. Wertheim, *J. Chem. Phys.* **90**, 2752 (1989).
- [9] J. R. Henderson, *Mol. Phys.* **59**, 89 (1986).
- [10] R. Kjellander and S. Sarman, *Mol. Phys.* **70**, 215 (1990).
- [11] L. Blum, D. Henderson, J. L. Lebowitz, C. Gruber, and P. A. Martin, *J. Chem. Phys.* **75**, 5974 (1981); L. Blum, C. Gruber, D. Henderson, J. L. Lebowitz, and P. A. Martin, *ibid.* **78**, 3195 (1983).
- [12] H. L. Friedman, *Ionic Solution Theory* (Wiley, New York, 1962).
- [13] D. Bratko, L. B. Bhuiyan, and C. W. Outhwaite, *J. Phys. Chem.* **90**, 6248 (1986).
- [14] R. Kjellander and S. Marčelja, *Chem. Phys. Lett.* **112**, 49 (1984); *J. Chem. Phys.* **82**, 2122 (1985).
- [15] A. S. Usenko, *Mol. Phys.* **71**, 721 (1990); E. Gonzales-Tovar, M. Lozada-Cassou, and W. Olivares, *J. Chem. Phys.* **94**, 2219 (1991).
- [16] V. Ya. Anthonchenko, V. V. Ilyin, N. N. Makovsky, and V. M. Khryapa, *Mol. Phys.* **65**, 117 (1988).
- [17] J. E. Mayer, *J. Chem. Phys.* **15**, 187 (1947); F. H. Stillinger and F. P. Buff, *ibid.* **37**, 1 (1962); J. L. Lebowitz and J. K. Percus, *J. Math. Phys.* **4**, 116 (1963); **4**, 1495 (1963).
- [18] B. Jancovici, *J. Stat. Phys.* **28**, 43 (1982).
- [19] B. Jancovici, *J. Stat. Phys.* **29**, 263 (1982).
- [20] D. A. McQuarrie, *Statistical Mechanics* (Harper&Row, New York, 1976).
- [21] J. P. Valleau and L. K. Cohen, *J. Chem. Phys.* **72**, 5935 (1980).
- [22] V. Vlachy and A. D. J. Haymet, *J. Am. Chem. Soc.* **111**, 477 (1989).
- [23] D. Bratko, C. E. Woodward, and A. Luzar, *J. Chem. Phys.* **95**, 5318 (1991).
- [24] D. M. Heyes, M. Berber, and J. H. R. Clarke, *J. Chem. Soc., Faraday II* **73**, 1485 (1977).
- [25] H. Totsuji, *J. Phys. C* **19**, L573 (1986).
- [26] Y. J. Rhee, J. W. Halley, J. Hautman, and A. Rahman, *Phys. Rev. B* **40**, 40 (1989).
- [27] D. Bratko, L. Blum, and L. B. Bhuiyan, *J. Chem. Phys.* **94**, 586 (1991).
- [28] D. N. Card and J. P. Valleau, *J. Chem. Phys.* **52**, 6232 (1970).
- [29] M. P. Allen and D. J. Tildesley, *Computer Simulation of Liquids* (Clarendon, Oxford, 1989).
- [30] B. R. Swenson and C. E. Woodward, *Mol. Phys.* **64**, 247 (1988).
- [31] L. B. Bhuiyan, D. Bratko, and C. W. Outhwaite, *J. Phys. Chem.* **95**, 336 (1991).
- [32] W. W. Wood, in *Physics of Simple Liquids*, edited by H. N. V. Temperley, G. S. Rushbrooke, and J. S. Rowlinson (North-Holland, Amsterdam, 1968), Chap. 5.
- [33] G. Karlström, *Chem. Scr.* **25**, 89 (1985).
- [34] M. Plischke and D. Henderson, *Proc. R. Soc. London Ser. A* **404**, 323 (1986).